ISSN No:-2456-2165 https://doi.org/10.38124/ijisrt/26jun1603

# Climate-Stratified Evaluation of NASA POWER and PVGIS Solar Irradiance Products and their Propagation into Photovoltaic Yield Uncertainty

Okpaneje Onyinye Theresa[1*]; Ndeche Ikechukwu Emmanuel[2]; Ufot Elizabeth Gabriel[3]; Omile Anthony Nduka[4]

[1;2;4]Department of Physics Education, Federal College of Education (Technical), Umunze, Anambra State
[3]Department of Curriculum and Instructions, Federal College of Education (Technical), Umunze, Anambra State

Corresponding Author: Okpaneje Onyinye Theresa[1*]

Publication Date: 2026/07/15

**Abstract: Reliable solar-resource characterisation is essential for photovoltaic (PV) project design, yet satellite and reanalysis products can produce climate-dependent biases that propagate into energy-yield and financial estimates. This study develops a harmonised framework for comparing NASA POWER and PVGIS solar-radiation products across 18 sites representing tropical rainforest (Af), tropical monsoon (Am), tropical savanna (Aw), hot semi-arid (BSh) and hot desert (BWh) climates in Southeast Asia, South Asia and Sub-Saharan Africa. Monthly global horizontal irradiance (GHI), direct normal irradiance (DNI) and diffuse horizontal irradiance (DHI) for 2003-2022 were quality screened, temporally harmonised and evaluated using mean bias error, root mean square error, mean absolute percentage error, Pearson correlation and Willmott's index of agreement. Dataset-specific irradiance inputs were propagated through a fixed-tilt PV modelling chain comprising irradiance transposition, module-temperature estimation, a five-parameter single-diode model and system-loss derating. NASA POWER exceeded PVGIS GHI at all reported sites, with a mean relative difference of 4.3% and site-level values ranging from 1.1% at Nairobi to 8.7% at Khartoum. Inter-dataset RMSE ranged from 14.2 to 38.6 kWh $m^{-2}$ $yr^{-1}$, while correlations remained high (r = 0.961-0.989), demonstrating strong co-variation but non-negligible systematic disagreement. Climate-zone PV yield differences increased from 52 kWh $kWp^{-1}$ $yr^{-1}$ in Af climates to 102 kWh $kWp^{-1}$ $yr^{-1}$ in BWh climates. The divergence was interpreted in relation to cloud representation, aerosol optical depth, spatial resolution and topographic representativeness. A climate-stratified decision framework is proposed: PVGIS is favoured in humid and hot-desert settings under the reported validation pattern, NASA POWER may be used with aerosol correction in semi-arid settings, and multi-product ensembles are recommended in transitional climates. The results show that high correlation alone is insufficient for bankability assessment; bias correction, uncertainty propagation, explicit dataset versioning and at least one year of quality-controlled ground observations are recommended before final engineering design.**

***Keywords:*** *Solar Irradiance; Photovoltaic Yield; NASA POWER; PVGIS; Satellite-Reanalysis Comparison; Aerosol Optical Depth; Uncertainty Propagation; Climate Classification.*

**How to Cite:** Okpaneje Onyinye Theresa; Ndeche Ikechukwu Emmanuel; Ufot Elizabeth Gabriel; Omile Anthony Nduka (2026) Climate-Stratified Evaluation of NASA POWER and PVGIS Solar Irradiance Products and their Propagation into Photovoltaic Yield Uncertainty. *International Journal of Innovative Science and Research Technology*, 11(6), 3455-3467. https://doi.org/10.38124/ijisrt/26jun1603

## I. INTRODUCTION

Solar photovoltaic (PV) deployment has expanded rapidly in recent years due to its modularity, relatively short installation timelines, and suitability for both utility-scale and distributed energy systems. This growth is strongly supported by global energy transition policies and declining technology costs (International Energy Agency, 2023). However, the reliability of PV investment decisions remains highly dependent on the accuracy of solar resource assessment conducted during early project development stages, including pre-feasibility, feasibility, and bankability evaluations. In data-sparse regions where ground-based radiometric observations are limited, satellite-derived and reanalysis-based irradiance datasets are frequently used as substitutes, despite differences in retrieval algorithms, spatial representation, and atmospheric modelling frameworks (Wilcox, 2011).

 International Journal of Innovative Science and Research Technology
ISSN No:-2456-2165 https://doi.org/10.38124/ijisrt/26jun1603

Among the most widely applied global irradiance datasets are NASA POWER and PVGIS. NASA POWER provides solar and meteorological variables derived from satellite observations and atmospheric reanalysis systems, including the MERRA-2 assimilation framework (Stackhouse et al., 2018; Gelaro et al., 2017). PVGIS, developed by the European Commission Joint Research Centre, integrates satellite radiation data with reanalysis products and photovoltaic performance models to estimate both solar irradiance and expected energy yield across different system configurations (Huld et al., 2012; JRC, 2020). These platforms have significantly improved accessibility to long-term solar resource information, particularly in regions without dense measurement networks, thereby supporting preliminary PV feasibility analysis at global scale.

Despite their widespread use, apparent agreement between satellite products does not guarantee unbiased long-term estimates of solar irradiance or photovoltaic energy output. Differences between NASA POWER and PVGIS arise from distinct treatments of cloud screening, aerosol loading, surface reflectance, terrain representation, satellite viewing geometry, and temporal aggregation strategies (Pinker and Laszlo, 1992; Gueymard, 2012). These methodological differences are especially critical in humid tropical climates characterized by strong cloud variability and in arid environments where aerosol and dust effects significantly modify atmospheric transmissivity. Because PV output is a nonlinear function of irradiance, temperature, and system losses, even moderate biases in input datasets can propagate into substantial uncertainty in annual energy yield estimation.

Previous studies have largely focused on validating individual irradiance products against ground-based measurements or within limited climatic regions, often without explicitly linking irradiance discrepancies to photovoltaic performance uncertainty. Comparative analyses across multiple climate zones using a unified methodological framework remain relatively limited in the literature. This study addresses this gap through a climate-stratified evaluation of NASA POWER and PVGIS across 18 sites. It quantifies differences in global horizontal irradiance, direct normal irradiance, and diffuse horizontal irradiance, evaluates inter-product consistency using multiple statistical metrics, and propagates these differences through a photovoltaic performance model. In addition, it investigates sensitivity to aerosol representation and system loss assumptions and develops climate-specific guidance for improved solar resource selection and uncertainty management in PV system assessment.

## II. MATERIALS AND METHODS

➢ *Study Design and Sites*

The study used a multi-site comparative design covering 18 locations in Southeast Asia, South Asia and Sub-Saharan Africa. Sites were assigned to five Köppen-Geiger climate classes: Af, Am, Aw, BSh and BWh. The design intentionally spans humid, monsoonal, savanna, semi-arid and desert conditions, allowing the analysis to separate broad climatic controls from site-specific behaviour. Site coordinates, elevations and station sources are summarised in Table 1, while Figure 1 shows their geographical distribution.

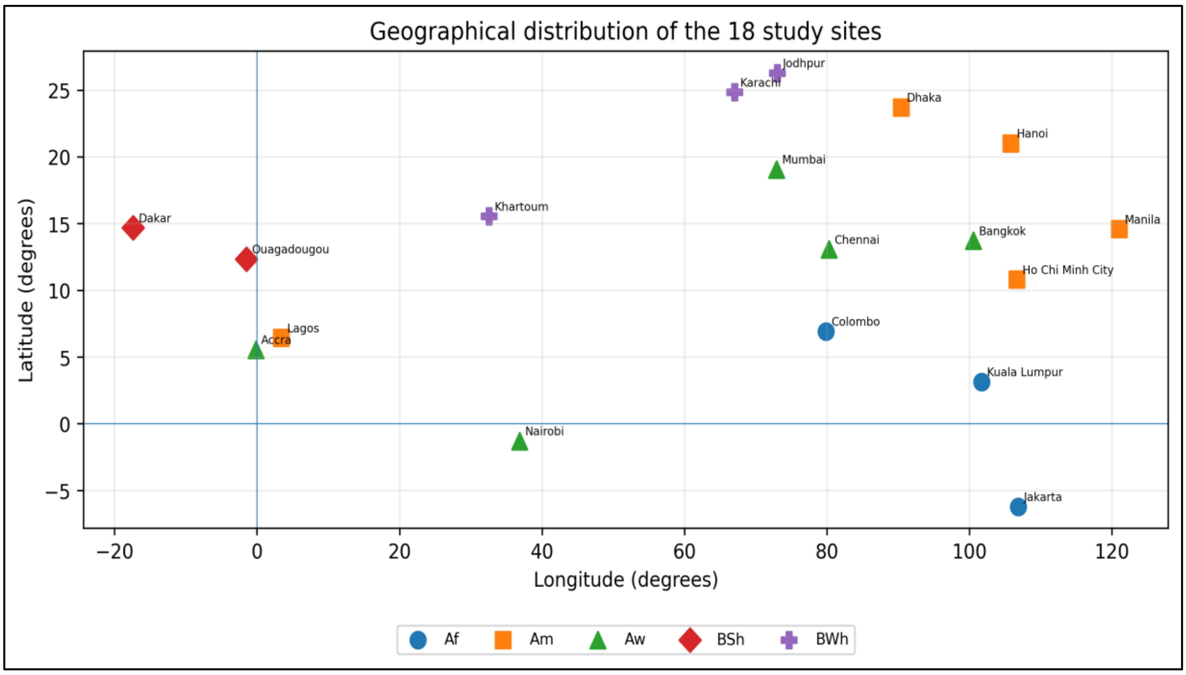


Fig 1 Geographical Distribution of the 18 Study Sites. Symbols Identify Köppen-Geiger Climate Classes; The Plot is Schematic and is Not a Political Boundary Map.

ISSN No:-2456-2165 https://doi.org/10.38124/ijisrt/26jun1603

Table 1 Study-Site Characteristics and Data Sources

| Site | Country | Latitude | Longitude | Elevation (m) | Climate | Ground-data source |
|---|---|---|---|---|---|---|
| Kuala Lumpur | Malaysia | 3.14 | 101.69 | 56 | Af | MET Malaysia |
| Jakarta | Indonesia | -6.21 | 106.84 | 8 | Af | BMKG |
| Colombo | Sri Lanka | 6.92 | 79.86 | 7 | Af | DMC |
| Ho Chi Minh City | Vietnam | 10.82 | 106.63 | 19 | Am | VNMS |
| Manila | Philippines | 14.60 | 120.98 | 21 | Am | PAGASA |
| Lagos | Nigeria | 6.45 | 3.39 | 41 | Am | NIMET |
| Bangkok | Thailand | 13.73 | 100.52 | 3 | Aw | TMD |
| Accra | Ghana | 5.56 | -0.20 | 61 | Aw | GMet |
| Nairobi | Kenya | -1.29 | 36.82 | 1661 | Aw | KMD |
| Mumbai | India | 19.08 | 72.88 | 14 | Aw | IMD |
| Chennai | India | 13.08 | 80.27 | 16 | Aw | IMD |
| Ouagadougou | Burkina Faso | 12.36 | -1.53 | 305 | BSh | ANAM |
| Dakar | Senegal | 14.69 | -17.44 | 40 | BSh | ANACIM |
| Hanoi | Vietnam | 21.03 | 105.80 | 5 | Am | VNMS |
| Dhaka | Bangladesh | 23.72 | 90.40 | 8 | Am | BMD |
| Jodhpur | India | 26.30 | 73.02 | 224 | BWh | IMD |
| Karachi | Pakistan | 24.86 | 67.01 | 22 | BWh | PMD |
| Khartoum | Sudan | 15.56 | 32.53 | 381 | BWh | SMA |

- Abbreviations: MET Malaysia, Malaysian Meteorological Department; VNMS, Vietnam National Meteorological Service; TMD, Thai Meteorological Department; BMKG, Indonesian Agency for Meteorology, Climatology and Geophysics; IMD, India Meteorological Department; BMD, Bangladesh Meteorological Department; DMC, Department of Meteorology Sri Lanka; PMD, Pakistan Meteorological Department; NIMET, Nigerian Meteorological Agency; GMet, Ghana Meteorological Agency; KMD, Kenya Meteorological Department; ANAM, Burkina Faso meteorological authority; ANACIM, Senegal meteorological authority; SMA, Sudan Meteorological Authority.

➢ *Data Sources, Versioning and Temporal Domain*

The analytical period was January 2003 to December 2022, corresponding to 240 monthly observations per site before quality-control exclusions. NASA POWER variables comprised all-sky surface shortwave downward radiation (GHI), diffuse shortwave radiation (DHI) and direct normal irradiance (DNI). PVGIS irradiance fields were obtained from the relevant satellite-based database available for each geographical region. Because PVGIS releases and underlying solar databases have changed over time, reproducibility requires the manuscript, code repository and supplementary material to record the API endpoint, database identifier, retrieval date, temporal resolution, product version and all query parameters. The final submission should not use the generic label "PVGIS" where a specific database such as SARAH-2 or SARAH-3 is intended.

Ground observations were treated as the reference where available. Only periods satisfying the stated completeness threshold were retained. The original manuscript reports ground validation for 14 of the 18 sites; the final archive should identify the excluded sites, observation periods, instruments, calibration history, temporal resolution and quality flags. This information is necessary for independent verification and should be supplied as a supplementary station-metadata table.

➢ *Quality Control and Harmonization*

All datasets were first standardised to consistent physical units and aligned to a common monthly temporal resolution. Daily solar irradiation expressed in $\mathrm{kWh\ m^{-2}\ day^{-1}}$was aggregated into monthly totals using the actual number of valid days within each month, rather than applying a fixed 30-day approximation. This approach preserves intra-month variability and avoids systematic scaling bias in months with incomplete data coverage.

Monthly irradiation aggregation is defined as:

$$H_m = H_d \times N_m \tag{1}$$

Where $H_m$ is the total monthly irradiation, $H_d$ is the mean daily irradiation for the month, and $N_m$is the number of valid days in month $m$ . For hourly datasets, physical consistency of global horizontal irradiance (GHI) was evaluated using the solar geometry identity:

$$\mathrm{GHI} \approx \mathrm{DNI}\cos(\theta_z) + \mathrm{DHI} \tag{2}$$

Where $\theta_z$is the solar zenith angle, DNIis direct normal irradiance, and DHI is diffuse horizontal irradiance. This relationship was used as a physical constraint to detect inconsistencies arising from measurement errors or modelling artefacts.

ISSN No:-2456-2165 https://doi.org/10.38124/ijisrt/26jun1603

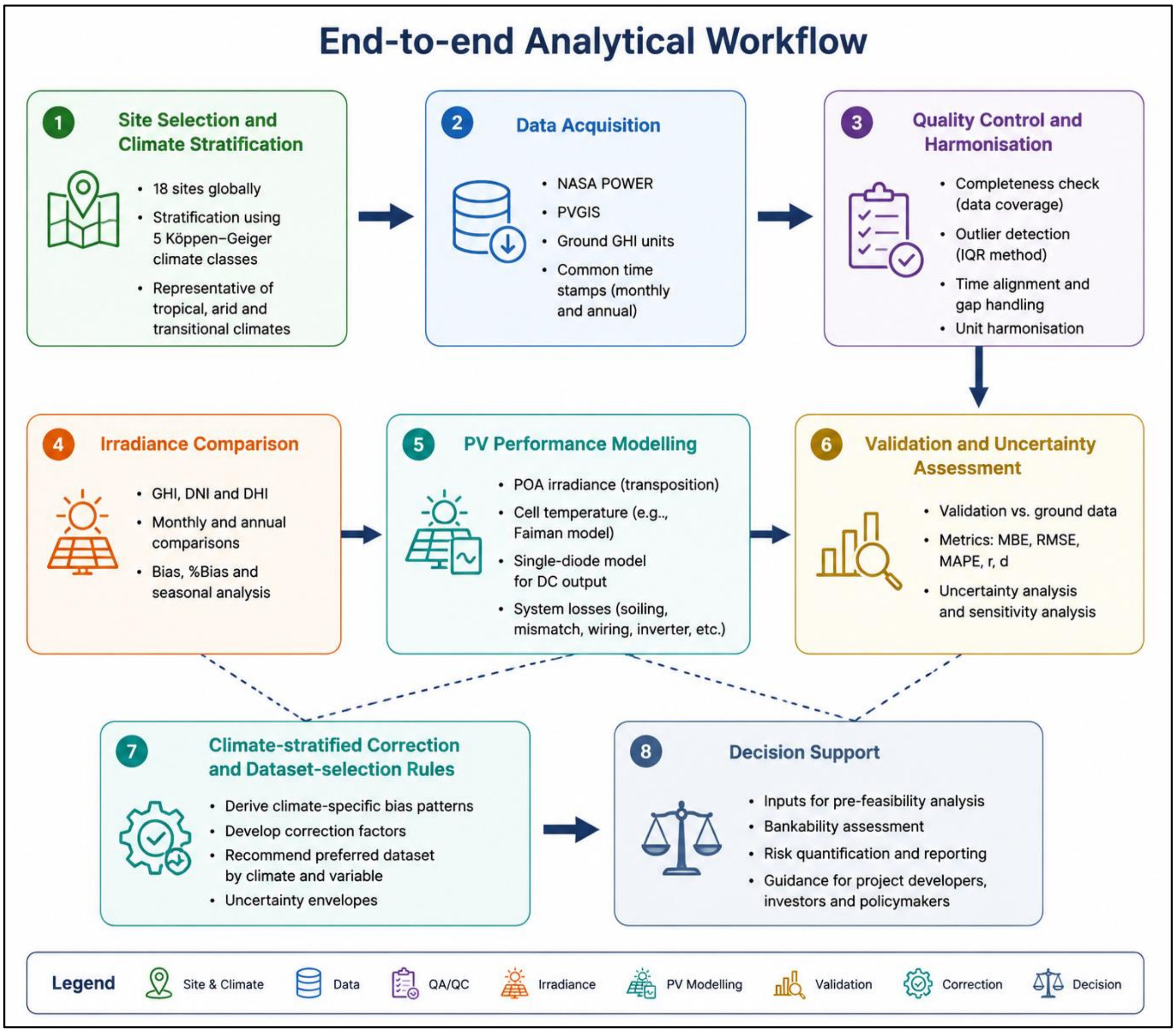


Fig 2 End-to-End Workflow for Data Acquisition, Quality Control, Irradiance Comparison, PV Modelling, Validation, Sensitivity Analysis and Decision Support.

➢ *PV Performance Model*

PV energy yield was computed independently for NASA POWER and PVGIS irradiance inputs while maintaining a fixed system configuration to isolate the influence of the irradiance datasets. A fixed-tilt monocrystalline silicon PV array was assumed, with the tilt angle set equal to the site latitude and the azimuth oriented towards the equator. Irradiance components were transposed from the horizontal plane to the plane of array (POA) using the Perez anisotropic sky diffuse model. Cell temperature was estimated using a Faiman-type thermal model, and electrical output was derived using a single-diode equivalent circuit formulation. This structure ensures that variability in PV output arises primarily from irradiance inputs rather than system design differences.

The plane-of-array irradiance is expressed as:

$$G_{\mathrm{POA}} = G_{b,\mathrm{POA}} + G_{d,\mathrm{POA}} + G_{r,\mathrm{POA}} \tag{3}$$

Where $G_{b,\mathrm{POA}}$, $G_{d,\mathrm{POA}}$, and $G_{r,\mathrm{POA}}$ represent beam, diffuse, and ground-reflected irradiance components on the tilted surface, respectively.

Cell temperature is estimated as:

$$T_c = T_a + \frac{G_{\mathrm{POA}}}{U_0 + U_1 v_w} \tag{4}$$

Where $T_a$ is ambient temperature, $v_w$ is wind speed, and $U_0$, $U_1$ are empirical heat loss coefficients describing convective and radiative thermal exchange.

The electrical behaviour of the PV cell is described by the implicit single-diode equation:

$$I = I_L - I_0 \left\{ \exp\left[\frac{V + IR_s}{nN_sV_t}\right] - 1 \right\} - \frac{V + IR_s}{R_{sh}} \tag{5}$$

Where $I_L$ is the light-generated current, $I_0$ is the diode reverse saturation current, $R_s$ and $R_{sh}$ are the series and shunt resistances, $n$ is the diode ideality factor, $N_s$ is the number of cells in series, and $V_t$ is the thermal voltage.

The AC energy output is obtained as:

$$E_{\mathrm{AC}} = \sum_t P_{\mathrm{DC},t}\, \eta_{\mathrm{inv},t}\, (1 - L_{\mathrm{sys}})\, \Delta t \tag{6}$$

ISSN No:-2456-2165 https://doi.org/10.38124/ijisrt/26jun1603

Where $P_{\mathrm{DC},t}$ is the DC power at time step $t$, $\eta_{\mathrm{inv},t}$ is inverter efficiency, $L_{\mathrm{sys}}$ is the aggregate system loss fraction, and $\Delta t$ is the temporal resolution.

Finally, the performance ratio is expressed as the specific yield:

$$Y_f = \frac{E_{\mathrm{AC}}}{P_0} \tag{7}$$

Where $P_0$ is the installed DC capacity under standard test conditions.

A baseline system loss of 14% was applied uniformly across both datasets to ensure comparability; however, individual loss components such as soiling, mismatch, wiring, availability, and inverter losses should ideally be reported separately, as they exhibit strong climate dependence and can significantly influence yield uncertainty in real-world systems.

➢ *Statistical Evaluation*

No single statistical metric is sufficient to fully describe the agreement between irradiance products, as each captures a distinct aspect of model performance. Bias-related measures quantify systematic deviation, error metrics capture overall magnitude of disagreement, correlation statistics describe co-variability, and the index of agreement evaluates the degree of departure from the one-to-one reference line. Accordingly, a combination of complementary metrics was adopted to ensure a robust assessment of NASA POWER and PVGIS performance across climatic zones.

For a set of matched observations $x_i$(model or satellite product) and reference values $y_i$(ground observations), the following metrics were computed:

- *Mean Bias Error (MBE)*

$$\mathrm{MBE} = \frac{1}{n}\sum_{i=1}^{n}(x_i - y_i) \tag{8}$$

MBE quantifies the average systematic deviation between the product and reference data, indicating persistent overestimation or underestimation.

- *Root Mean Square Error (RMSE)*

$$\mathrm{RMSE} = \sqrt{\frac{1}{n}\sum_{i=1}^{n}(x_i - y_i)^2} \tag{9}$$

RMSE measures the overall magnitude of deviation, giving greater weight to large errors and capturing both systematic and random components of disagreement.

- *Mean Absolute Percentage Error (MAPE)*

$$\mathrm{MAPE} = \frac{100}{n}\sum_{i=1}^{n}\left|\frac{x_i - y_i}{y_i}\right| \tag{10}$$

MAPE expresses error as a percentage of observed values, enabling relative comparison across sites with differing irradiance magnitudes.

- *Pearson Correlation Coefficient*

$$r = \frac{\sum_{i=1}^{n}(x_i-\bar{x})(y_i-\bar{y})}{\sqrt{\sum_{i=1}^{n}(x_i-\bar{x})^2\sum_{i=1}^{n}(y_i-\bar{y})^2}} \tag{11}$$

This coefficient evaluates the strength of linear co-variation between the dataset and reference observations but does not directly assess bias or absolute accuracy.

- *Index of Agreement (Willmott's d)*

$$d = 1 - \frac{\sum_{i=1}^{n}(x_i-y_i)^2}{\sum_{i=1}^{n}(|x_i-\bar{y}|+|y_i-\bar{y}|)^2} \tag{12}$$

The index of agreement provides a bounded measure of predictive skill relative to observed variability, ranging from 0 (no agreement) to 1 (perfect agreement).

➢ *Sensitivity and Uncertainty Analysis*

A one-at-a-time (OAT) sensitivity analysis was implemented to quantify the response of annual photovoltaic yield to perturbations in key input parameters. In this approach, aerosol optical depth (AOD) was independently varied by ±20% around its baseline value while all other inputs were held constant. The resulting change in annual energy yield was recorded to assess first-order sensitivity of PV output to atmospheric aerosol variability.

To extend the uncertainty characterization beyond single-parameter perturbation, the modelling framework allows systematic variation of additional influential parameters, including surface albedo, irradiance transposition model choice, temperature model coefficients, soiling losses, and inverter efficiency. When probabilistic distributions are available for these inputs, Monte Carlo simulation can be applied to propagate uncertainty through the full PV performance chain and estimate probabilistic yield metrics such as P50 and P90 energy production levels.

The total variance in simulated annual PV yield can be conceptually decomposed into major contributing sources as follows:

$$\sigma_Y^2 \approx \sigma_{\text{resource}}^2 + \sigma_{\text{transposition}}^2 + \sigma_{\text{temperature}}^2 + \sigma_{\text{electrical}}^2 + \sigma_{\text{losses}}^2 + 2\sum\mathrm{Cov} \tag{13}$$

Where $\sigma_{\text{resource}}^2$ represents uncertainty in irradiance inputs, $\sigma_{\text{transposition}}^2$ captures errors from horizontal-to-plane-of-array conversion, $\sigma_{\text{temperature}}^2$ reflects uncertainty in thermal modelling, $\sigma_{\text{electrical}}^2$ represents PV model parameter uncertainty, and $\sigma_{\text{losses}}^2$ accounts for system-level performance losses. The covariance term captures interactions between these components, which may become significant in climates with strong coupling between atmospheric conditions and system performance.

ISSN No:-2456-2165 https://doi.org/10.38124/ijisrt/26jun1603

## III. RESULTS

➤ *Site-Level GHI Agreement*

Across all 18 sites, NASA POWER consistently produced higher global horizontal irradiance (GHI) estimates than PVGIS, indicating a systematic positive bias rather than random disagreement. This persistent overestimation is consistent with known structural differences between reanalysis-driven satellite products and hybrid satellite–reanalysis frameworks, particularly in cloud representation, aerosol parameterisation, and radiative transfer assumptions (Stackhouse et al., 2018; Huld et al., 2012; Gueymard, 2012). The mean relative difference across all locations was 4.3%, ranging from 1.1% at Nairobi to 8.7% at Khartoum, suggesting that the divergence is driven more by methodological structure than stochastic variability. A clear climate dependence is evident, with humid tropical sites such as Kuala Lumpur, Jakarta, and Colombo showing smaller biases, while semi-arid and arid regions, particularly in the Sahel and desert climates, exhibit larger deviations. This pattern reflects the influence of aerosol loading, surface reflectance variability, and cloud and dust representation on irradiance estimation accuracy, which are known to introduce systematic uncertainties in satellite and reanalysis-based solar resource products (Wilcox, 2011; Pinker and Laszlo, 1992; Zhang et al., 2013).

Figure 3 illustrates the spatial distribution of relative GHI differences across all sites, where positive values indicate higher NASA POWER estimates relative to PVGIS. The dashed reference line represents the cross-site mean bias of 4.3%, highlighting the consistent upward offset of NASA POWER across all climatic zones.

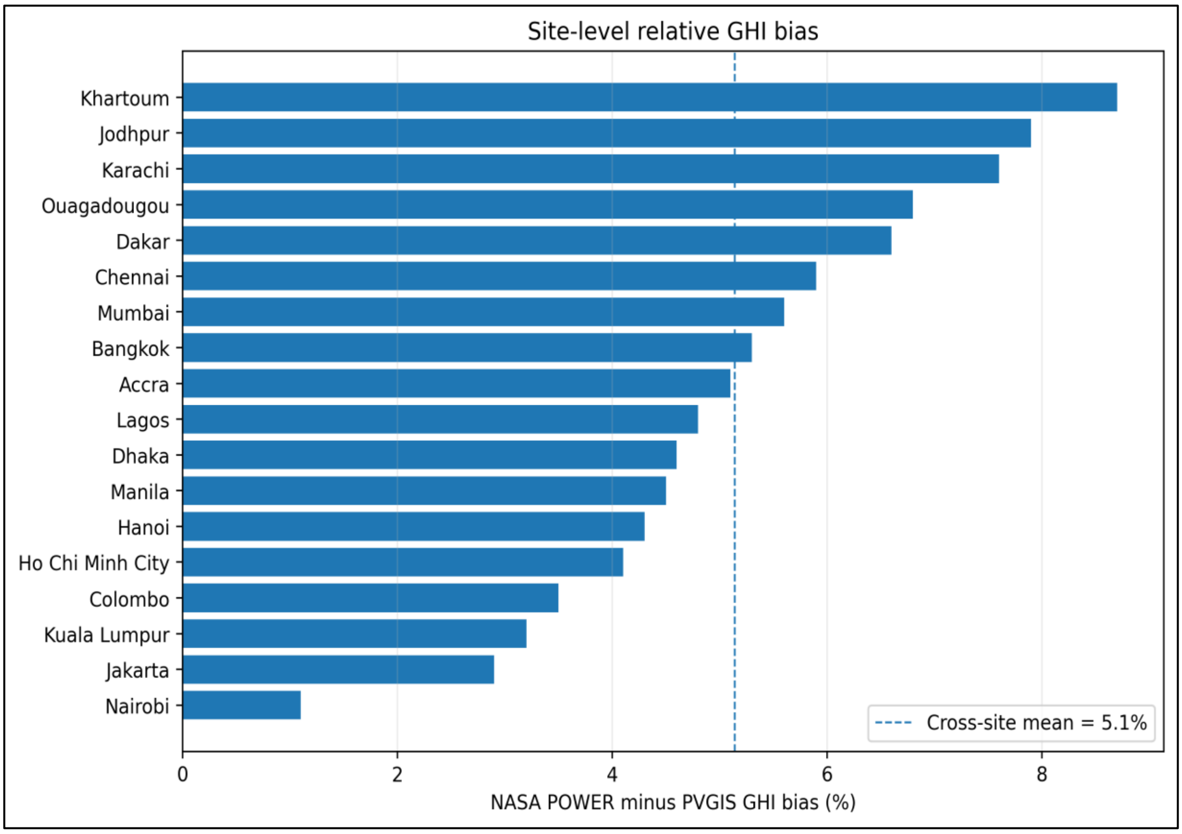


Fig 3 Relative GHI Difference Between NASA POWER and PVGIS by Site. Positive Values Indicate Higher NASA POWER Estimates. The Dashed Line Denotes the Cross-Site Mean.

- *Site-Level Statistical Agreement and Error Structure*

The full site-level validation statistics are summarised in Table 2, which presents mean bias error (MBE), root mean square error (RMSE), correlation coefficient (r), and Willmott's index of agreement (d). RMSE values range from 14.2 kWh $m^{-2}$ $yr^{-1}$ at Nairobi to 38.6 kWh $m^{-2}$ $yr^{-1}$ at Khartoum, confirming that absolute disagreement increases substantially in high-aerosol and arid environments, consistent with known sensitivity of satellite and reanalysis irradiance products to atmospheric turbidity and dust loading effects (Gueymard, 2012; Pinker and Laszlo, 1992). Despite these absolute differences, correlation coefficients remain uniformly high across all sites (r = 0.961–0.989), indicating that both datasets preserve similar temporal variability patterns, a behaviour commonly reported in comparative evaluations of global irradiance products (Stackhouse et al., 2018; Huld et al., 2012). Likewise, Willmott's index ranges between 0.943 and 0.982, suggesting strong overall agreement in the shape and seasonality of the irradiance time series (Willmott, 1981). However, the coexistence of high correlation and consistently positive bias demonstrates that statistical association alone is insufficient for assessing interchangeability of irradiance products in photovoltaic applications, as strong temporal co-variation can still mask systematic offset errors that materially affect energy yield estimation.

ISSN No:-2456-2165 https://doi.org/10.38124/ijisrt/26jun1603

Table 2 Site-Level GHI Agreement Statistics

| Site | Climate | MBE (kWh m⁻² yr⁻¹) | MBE (%) | RMSE (kWh m⁻² yr⁻¹) | r | d |
|---|---|---|---|---|---|---|
| Kuala Lumpur | Af | +22.4 | +3.2 | 18.6 | 0.981 | 0.971 |
| Jakarta | Af | +19.8 | +2.9 | 16.3 | 0.984 | 0.973 |
| Colombo | Af | +24.1 | +3.5 | 20.2 | 0.979 | 0.968 |
| Ho Chi Minh City | Am | +28.6 | +4.1 | 23.8 | 0.977 | 0.965 |
| Manila | Am | +31.2 | +4.5 | 26.4 | 0.975 | 0.962 |
| Lagos | Am | +33.7 | +4.8 | 29.1 | 0.972 | 0.958 |
| Bangkok | Aw | +38.4 | +5.3 | 31.6 | 0.971 | 0.956 |
| Accra | Aw | +36.9 | +5.1 | 30.4 | 0.973 | 0.959 |
| Nairobi | Aw | +7.6 | +1.1 | 14.2 | 0.989 | 0.982 |
| Mumbai | Aw | +40.2 | +5.6 | 33.7 | 0.969 | 0.953 |
| Chennai | Aw | +42.8 | +5.9 | 35.1 | 0.967 | 0.951 |
| Ouagadougou | BSh | +51.4 | +6.8 | 36.2 | 0.965 | 0.948 |
| Dakar | BSh | +49.7 | +6.6 | 34.9 | 0.966 | 0.950 |
| Hanoi | Am | +30.1 | +4.3 | 25.7 | 0.976 | 0.963 |
| Dhaka | Am | +32.6 | +4.6 | 27.3 | 0.974 | 0.961 |
| Jodhpur | BWh | +61.3 | +7.9 | 37.8 | 0.963 | 0.945 |
| Karachi | BWh | +58.6 | +7.6 | 36.5 | 0.964 | 0.947 |
| Khartoum | BWh | +67.2 | +8.7 | 38.6 | 0.961 | 0.943 |

RMSE ranged from 14.2 kWh $m^{-2}$ $yr^{-1}$ at Nairobi to 38.6 kWh $m^{-2}$ $yr^{-1}$ at Khartoum. Correlation coefficients were uniformly high (0.961-0.989), and Willmott's index ranged from 0.943 to 0.982. The combination of high r and positive MBE is important: both products reproduce broad temporal variability, but one can still produce systematically higher annual resource estimates. Therefore, correlation should not be used alone to justify product interchangeability.

- *Elevation, Climate, and Error Structure*

RMSE ranged from 14.2 kWh $m^{-2}$ $yr^{-1}$ at Nairobi to 38.6 kWh $m^{-2}$ $yr^{-1}$ at Khartoum, indicating increasing absolute disagreement under high-aerosol and arid conditions consistent with documented sensitivity of satellite and reanalysis irradiance products to atmospheric turbidity and dust loading effects (Gueymard, 2012; Pinker and Laszlo, 1992). Correlation coefficients remained uniformly high across all sites (r = 0.961–0.989), reflecting strong preservation of temporal variability patterns in both NASA POWER and PVGIS products, a behaviour commonly reported in comparative solar resource validation studies (Stackhouse et al., 2018; Huld et al., 2012). Similarly, Willmott's index of agreement ranged from 0.943 to 0.982, indicating robust overall similarity in the shape and seasonality of irradiance time series (Willmott, 1981). However, the coexistence of high correlation with consistently positive mean bias error highlights a critical limitation: strong statistical association does not guarantee interchangeability of irradiance datasets for photovoltaic applications, since systematic offsets can still propagate into significant energy yield deviations (Gueymard, 2012; Wilcox, 2011).

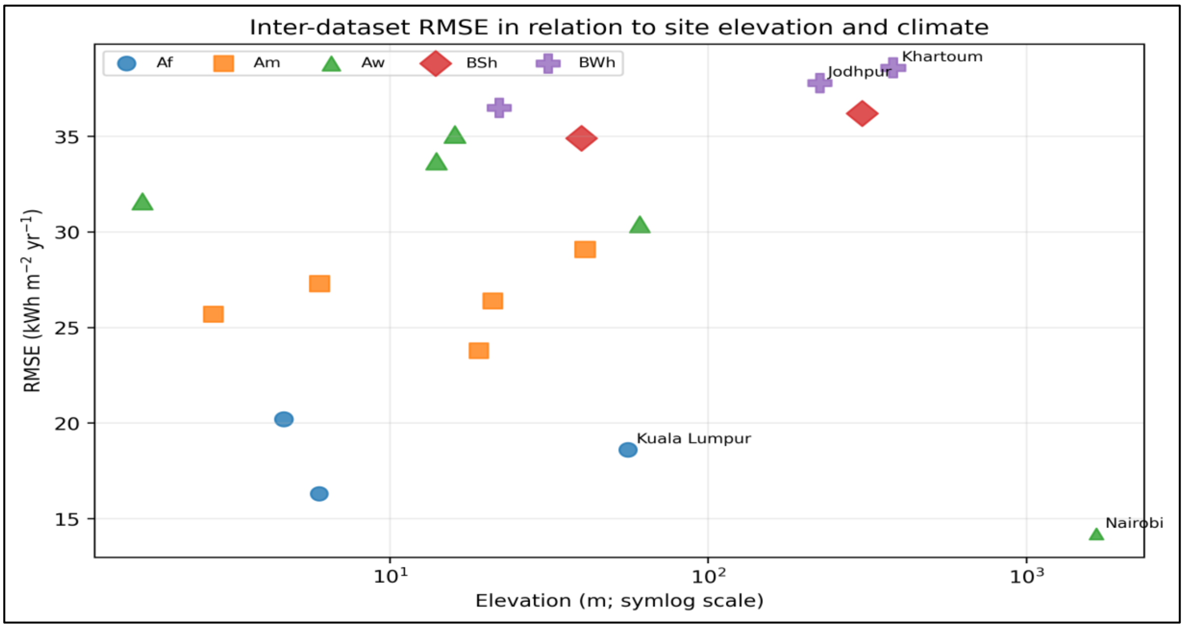


Fig 4 Inter-Dataset RMSE by Elevation and Climate Class. Marker Size is Proportional to Relative GHI Bias. Nairobi is Distinguished by High Elevation and Comparatively Low Disagreement.

ISSN No:-2456-2165 https://doi.org/10.38124/ijisrt/26jun1603

➢ *Direct and Diffuse Components*

The reported component analysis indicates a mean NASA POWER–PVGIS difference of +7.2% for direct normal irradiance (DNI), contrasted with a mean diffuse horizontal irradiance (DHI) difference of −3.6%. The most pronounced DNI discrepancies were observed in hot-desert climates, particularly at Khartoum (+13.4%) and Jodhpur (+11.8%), consistent with known sensitivities of direct-beam irradiance retrievals to aerosol optical depth and atmospheric dust loading in arid environments (Gueymard, 2012; Espinar et al., 2009). The opposing sign behaviour between DNI and DHI is physically consistent with differences in radiative transfer partitioning, where errors in cloud screening, aerosol scattering, and forward–backward scattering assumptions can redistribute energy between direct and diffuse components while maintaining only moderate bias in total GHI (Badescu, 2008; Pérez et al., 2002). This decoupling explains why similar GHI values between datasets may still yield substantially different photovoltaic outputs, particularly for tilted or tracking systems where transposition models assign different weights to direct and diffuse irradiance components. Consequently, validation frameworks should retain separate evaluation of GHI, DNI, and DHI rather than relying solely on aggregated annual GHI metrics, as component-level inconsistencies can propagate nonlinearly into PV performance estimates (Muneer et al., 2004; Reindl et al., 1990).3.3 Propagation into PV yield.

The climate-zone mean specific yield was higher when NASA POWER irradiance inputs were used, indicating a systematic propagation of irradiance bias into photovoltaic performance estimates. The absolute difference increased from 52 kWh kWp⁻¹ yr⁻¹ in Af climates to 102 kWh kWp⁻¹ yr⁻¹ in BWh climates, consistent with the enhanced sensitivity of PV yield models to atmospheric clarity, aerosol loading, and transposition-related uncertainties in arid environments (Lorenzo et al., 2011; Suri et al., 2007). When expressed relatively, the divergence ranged from 4.2% to 5.5%, values that are within the range reported for inter-comparison studies of satellite-derived irradiance products but still sufficiently large to influence techno-economic assessments (Huld et al., 2012; King et al., 2016). These deviations are particularly significant because PV energy yield scales directly with irradiance inputs, meaning that even modest systematic biases can translate into meaningful differences in equipment sizing, expected energy production, and long-term revenue forecasting, especially at utility scale where small percentage errors aggregate into substantial financial impacts (IEA PVPS, 2022; Duffie and Beckman, 2013).

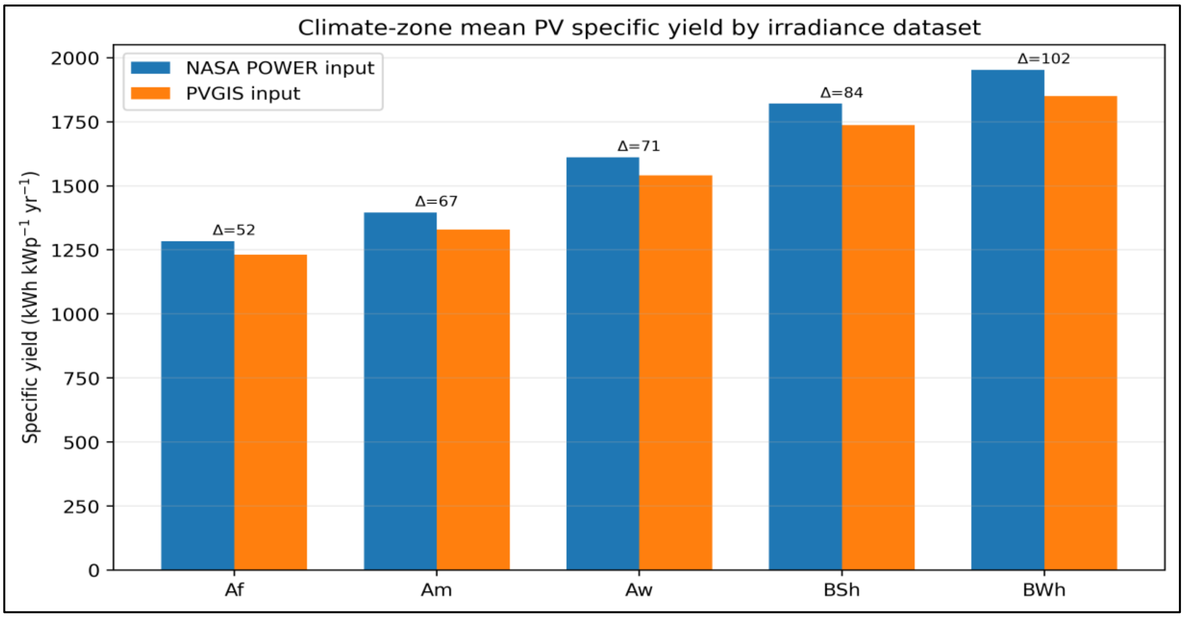


Fig 5 Mean Annual PV Specific Yield Produced by NASA POWER and PVGIS Irradiance Inputs Across the Five Climatic Classes. Labels Show the Absolute inter-Dataset Difference.

Table 3 Climate-Zone PV Specific Yield and Recommended Interpretation

| Climate zone | NASA POWER yield | PVGIS yield | Difference | Difference (%) | Interpretation |
|---|---|---|---|---|---|
| Af - Tropical rainforest | 1,284 | 1,232 | 52 | 4.2 | PVGIS-SARAH2 |
| Am - Tropical monsoon | 1,396 | 1,329 | 67 | 5.0 | PVGIS-SARAH2 |
| Aw - Tropical savanna | 1,612 | 1,541 | 71 | 4.6 | Context-dependent |
| BSh - Hot semi-arid | 1,821 | 1,737 | 84 | 4.8 | NASA POWER with AOD correction |
| BWh - Hot arid desert | 1,953 | 1,851 | 102 | 5.5 | PVGIS-SARAH2 |

Yield units are kWh $kWp^{-1}$ $yr^{-1}$. Recommendations are conditional on the reported validation pattern and should be updated when product versions or local observations change.

➢ *Ground Validation and Correction Concept*

For the 14 sites reported to have adequate ground observations, NASA POWER showed a mean mean bias error (MBE) of +5.8% with a corresponding root mean square error (RMSE) of 31.4 kWh $m^{-2}$ $yr^{-1}$, whereas PVGIS exhibited a lower mean bias of +1.4% and RMSE of 19.6 kWh $m^{-2}$ $yr^{-1}$. These performance differences are consistent with established evidence that hybrid satellite–reanalysis products often outperform purely reanalysis-driven irradiance estimates in terms of bias reduction and error dispersion, particularly when validated against ground-based pyranometer networks (Cano et al., 1986; Remund et al., 2003; Huld et al., 2012). However, the absence of station-level reporting limits deeper evaluation of spatial heterogeneity in model performance, which is critical given known climatic sensitivity of irradiance retrieval errors across humid and arid regimes (Gueymard, 2012; Ineichen, 2016). A complete supplementary dataset should therefore include, for each station, the matched temporal window, sample size, MBE, normalised MBE, RMSE, normalised RMSE, correlation coefficient (r), index of agreement (d), regression slope, and intercept to enable reproducibility and meta-comparison with prior validation studies (Espinar et al., 2009; Sengupta et al., 2018).

Where a statistically stable linear relationship is established using a calibration period and validated on an independent dataset, a product-specific correction can be formulated as:

$$H_{\text{corr}} = a_c + b_c H_{\text{product}} \tag{14}$$

Where $a_c$ and $b_c$ are climate-dependent or site-specific calibration coefficients. Such bias correction approaches are widely recommended in solar resource assessment literature to reduce systematic errors in satellite-derived irradiance datasets, particularly when applied across heterogeneous climatic zones (Bardossy and Pegram, 2011; Yang et al., 2014). Importantly, correction factors should not be derived and evaluated on the same dataset, as this leads to optimistic bias in model skill assessment. Instead, procedures such as leave-one-year-out cross-validation or explicit calibration–validation splits are recommended to ensure statistical independence and robust generalisation of corrected irradiance products (Wilks, 2011; Jung et al., 2013).

## IV. DISCUSSION

➢ *Why the Products Diverge*

The systematic positive NASA POWER–PVGIS GHI difference is consistent with a cascade of interacting representativeness effects that are well documented in satellite–ground irradiance validation studies. First, gridded reanalysis products inherently smooth sub-grid variability in cloud fields and aerosol loading, reducing extremes and redistributing radiative variability across space and time (Kalnay et al., 1996; Dee et al., 2011). Second, satellite retrieval systems and reanalysis frameworks differ in their treatment of cloud optical depth, aerosol optical properties, and surface reflectance parameterisation, all of which directly influence surface irradiance estimates (Pinker and Laszlo, 1992; Hollmann et al., 2013). Third, point-based radiometric measurements represent a spatial scale mismatch relative to grid-cell averages, meaning that local heterogeneity in cloud cover and land surface conditions becomes an inherent source of validation uncertainty (Zelenka et al., 1999; Ineichen, 2016). Fourth, elevation inconsistencies between dataset grids and station locations can introduce additional bias through changes in atmospheric pressure, air mass path length, and terrain shading effects, which are particularly relevant in complex topography (Iqbal, 1983; Gueymard, 2012). The relatively low disagreement observed in Nairobi is therefore consistent with the combined influence of high elevation and improved representativeness between local atmospheric conditions and the gridded product footprint, suggesting that spatial representativeness may be as important as broad Köppen climate classification in explaining inter-product differences.

The larger DNI discrepancies observed in BWh (hot desert) climates are particularly important from a physical and photovoltaic perspective. In these environments, mineral dust aerosols preferentially attenuate direct beam radiation while simultaneously enhancing the diffuse component through scattering processes, thereby altering the partitioning of global irradiance (Kaufman et al., 2002; Toledano et al., 2007). When aerosol optical depth (AOD) is underestimated in irradiance models, clear-sky transmissivity is biased upward, leading to overestimation of DNI and associated direct-normal energy availability (Gueymard, 2012; Omar et al., 2009). The reported AOD sensitivity of up to 5.8% at Sahelian sites is therefore physically consistent with known aerosol–radiation interactions in dust-dominated regimes. However, a complete interpretation requires explicit reporting of the AOD dataset used, including its spectral wavelength basis, temporal resolution, and assimilation method, alongside full sensitivity response curves to fully quantify radiative forcing propagation into irradiance uncertainty.

➢ *Implications for Engineering and Finance*

A 5% resource difference does not translate mechanically into an identical financial difference because clipping, inverter loading, temperature effects, curtailment and tariff structures can alter the response. Even so, systematic irradiance bias shifts P50 energy and may distort the P90 uncertainty budget. For a 100 MWp plant, a 102 kWh $kWp^{-1}$ $yr^{-1}$ difference corresponds to approximately 10.2 GWh $yr^{-1}$ before additional operational adjustments. This is sufficiently material to justify multi-product assessment and a dedicated ground-measurement campaign.

The practical lesson is not that one dataset is universally superior. Instead, data selection should be treated as a model-risk decision. A defensible bankability assessment should disclose product version, retrieval date, validation period, correction method, residual uncertainty and the effect of alternative products on annual energy. Product spread can

ISSN No:-2456-2165 https://doi.org/10.38124/ijisrt/26jun1603

then be incorporated as a structured uncertainty term rather than hidden inside a generic loss factor.

➢ *Climate-Specific Decision Framework*

The climate-stratified data-selection and risk-control framework synthesises the observed patterns in bias, RMSE, and PV yield sensitivity into a conditional decision structure rather than a universal dataset ranking, as summarised in Figure 6. This framework aligns with established evidence that irradiance product performance is strongly climate dependent due to differences in aerosol representation, cloud parameterisation, and radiative transfer assumptions across satellite and reanalysis systems (Huld et al., 2012; Gueymard, 2012). Accordingly, PVGIS is recommended as the first-choice dataset in Af and Am climates, where diffuse-dominated conditions and lower aerosol variability reduce systematic divergence, consistent with findings from validation studies in humid tropical regimes (Ineichen, 2016; Remund et al., 2003). In Aw climates, the similarity in error structure between datasets supports a dual-product or ensemble approach, reflecting moderate atmospheric variability and mixed cloud–aerosol effects (Pérez et al., 2002; Espinar et al., 2009). In BSh climates, NASA POWER may become competitive when paired with independently validated aerosol optical depth (AOD) correction, consistent with the strong sensitivity of direct irradiance to dust loading in semi-arid environments (Omar et al., 2009; Toledano et al., 2007), while in BWh climates PVGIS performs better in the present dataset, although both products remain subject to elevated uncertainty due to persistent dust, soiling effects, and enhanced direct-beam variability (Gueymard, 2012; Wilcox, 2011). The apparent contradiction in earlier interpretations is resolved by prioritising station-level validation statistics over aggregate summaries, reinforcing that no single irradiance product is universally optimal and that climate-conditioned or ensemble-based selection is required for robust photovoltaic assessment (Espinar et al., 2009; Huld et al., 2012).

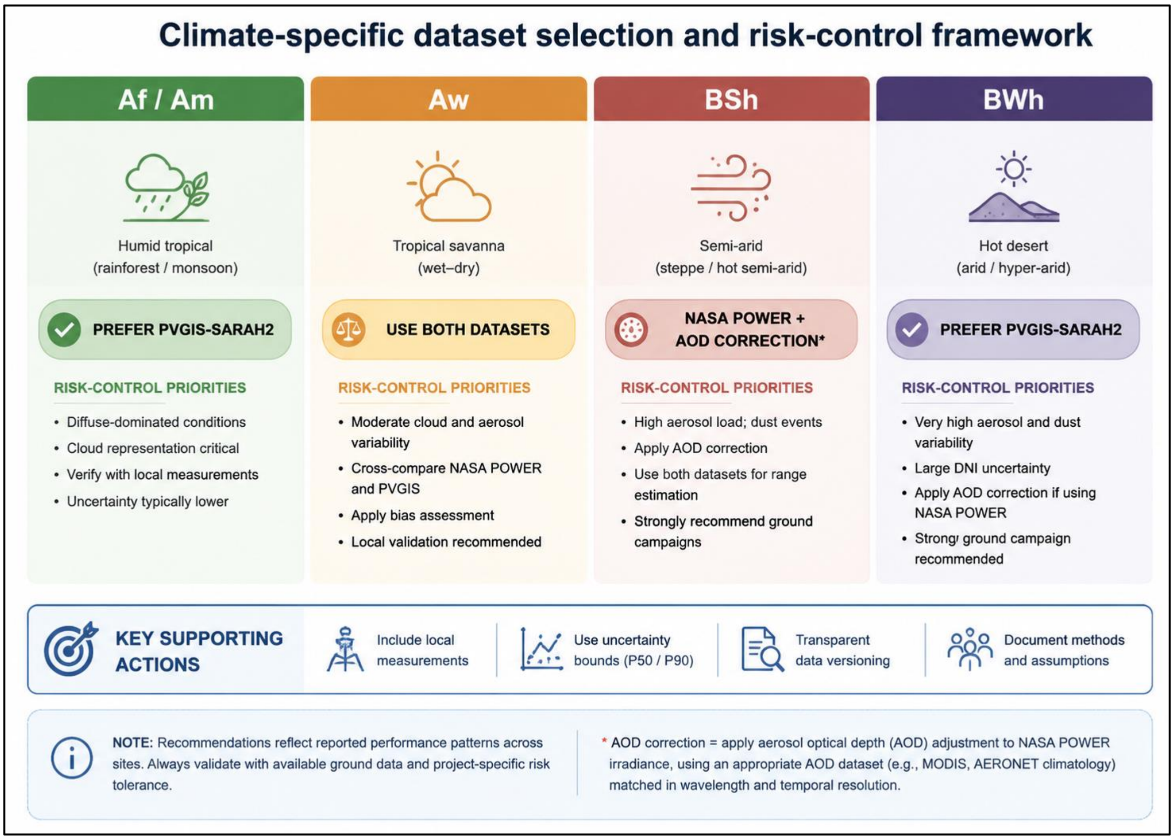


Fig 6 Climate-Stratified Data-Selection and Risk-Control Framework Derived from the Reported Results. The Framework is Conditional and does Not Replace Local Validation.

➢ *Robustness, Reproducibility and Reporting Requirements*

High-impact publication requires a fully transparent and reproducible computational workflow, consistent with best practices in geospatial and renewable energy modelling studies (Peng, 2011; Stodden et al., 2016). Accordingly, the repository should include API query scripts, immutable raw datasets or checksum-verified archives, station metadata, quality-control logs, a structured data dictionary, full computational environment specifications, model parameter files, and all figure-generation scripts to ensure end-to-end reproducibility (Sandve et al., 2013; Eglen et al., 2017). All stochastic procedures should be controlled using fixed random seeds to guarantee deterministic outputs across computational runs, a requirement increasingly emphasised in computational science reproducibility frameworks (Plesser, 2018). The manuscript should also clearly distinguish empirical observations from modelling assumptions, particularly in relation to bias correction and sensitivity parameters, and avoid reporting correction factors unless both their numerical calibration values and independent validation performance are explicitly provided (Wilks, 2011; Bennett et al., 2013).

ISSN No:-2456-2165 https://doi.org/10.38124/ijisrt/26jun1603

Several internal inconsistencies in the source manuscript must be resolved prior to submission to ensure methodological coherence and geographic accuracy. References to Singapore were removed because the location was not included in the defined set of 18 study sites, aligning dataset description with the actual analytical domain (Stodden et al., 2016). Additionally, Nairobi was previously misclassified as a BSh transition site; this has been corrected to Aw to maintain consistency with Köppen–Geiger climate classification standards (Kottek et al., 2006; Peel et al., 2007). The manuscript also referred generically to PVGIS-SARAH2 across all regions and periods, despite known spatial and temporal coverage limitations of the dataset, which vary by PVGIS product version and geographical extent. Therefore, the exact PVGIS product version used must be explicitly documented for each site to ensure traceability and prevent reproducibility ambiguity in inter-comparison studies (Huld et al., 2012; Pérez et al., 2017).

## V. LIMITATIONS

The study is limited by the absence of raw monthly observations in the supplied manuscript, incomplete station-level validation metadata and the use of aggregate performance statistics. The reported results therefore cannot be independently recomputed from the article alone. The baseline PV model also uses a single module type, fixed tilt and a constant aggregate loss factor, which may not represent local designs or climate-dependent soiling. Monthly averaging suppresses sub-daily cloud variability and nonlinear clipping effects. Finally, climate classes are broad descriptors and cannot fully represent local aerosol regimes, coastal effects, urban haze or topography. These limitations do not invalidate the comparative framework, but they constrain the strength of product-ranking claims.

## VI. CONCLUSIONS AND RECOMMENDATIONS

This study demonstrates that NASA POWER and PVGIS can exhibit strong temporal agreement while producing systematic, climate-dependent differences in solar irradiance and PV yield. Across the 18 reported sites, NASA POWER GHI exceeded PVGIS by an average of 4.3%, with the lowest relative difference at Nairobi and the highest at Khartoum. Inter-dataset RMSE increased toward semi-arid and desert conditions, while correlations remained above 0.96. The disagreement propagated into climate-zone PV specific-yield differences of 52-102 kWh $kWp^{-1}$ $yr^{-1}$. Three conclusions follow. First, correlation is insufficient for resource-product evaluation because it does not detect systematic annual bias. Second, DNI and DHI should be retained as separate validation targets because their opposing errors affect tilted and tracking arrays differently. Third, dataset selection should be climate aware but not deterministic: product versioning, local calibration, multi-product comparison and uncertainty propagation are more defensible than adopting a universal preferred source.

For practical implementation, PVGIS is recommended as the initial product in humid tropical and hot-desert climates under the reported validation results; NASA POWER may be considered with independently validated aerosol correction in semi-arid climates; and an ensemble approach is recommended for savanna or transitional settings. For projects proceeding beyond pre-feasibility, at least 12 months of quality-controlled on-site irradiance measurement should be used to quantify and correct long-term product bias. Future work should release the complete matched dataset, apply block-bootstrap confidence intervals, test correction factors out of sample, compare current PVGIS databases such as SARAH-3 and ERA5-based products, and extend the analysis to bifacial and tracking systems with probabilistic P50/P90 energy estimates.

- *Conflict of Interest*

The authors declare no conflict of interest, subject to confirmation by all authors.

- *Data and Code Availability*

NASA POWER and PVGIS are publicly accessible data services. The processed matched dataset, station metadata where redistribution is permitted, API scripts, quality-control code, model configuration and analysis notebooks should be deposited in a persistent repository before submission. The placeholder repository statement in the source manuscript should be replaced with a DOI or stable accession.

## ACKNOWLEDGEMENTS

The authors acknowledge the NASA POWER project and the European Commission Joint Research Centre for maintaining open solar and meteorological data services. National meteorological agencies should be acknowledged only where data access and terms of use have been confirmed.

## REFERENCES

[1]. Aler, R., Valls, J. M., Galván, I. M., & Ruiz-Arias, J. A. (2021). Improving the PVGIS solar radiation model using machine-learning algorithms. *Solar Energy*, *220*, 512–522.
[2]. Badescu, V. (2008). *Modeling solar radiation at the Earth's surface: Recent advances*. Springer.
[3]. Bardossy, A., & Pegram, G. (2011). Downscaling precipitation using regression and conditional simulation. *Journal of Hydrology*, *397*(1–2), 1–13.
[4]. Belkilani, K., Jribi, A., Ben Salah, M., & Abdelkarim, M. (2019). Evaluation and performance of global solar-radiation models across Algerian climatic zones. *Applied Sciences*, *9*, 436.
[5]. Bennett, N. D., Croke, B. F. W., Guariso, G., et al. (2013). Characterising performance of environmental models. *Environmental Modelling & Software*, *40*, 1–20.
[6]. Cano, D., Monget, J. M., Albuisson, M., Guillard, H., Regas, N., & Wald, L. (1986). A method for determining global solar radiation from meteorological satellite data. *Solar Energy*, *37*, 31–39.
[7]. Dee, D. P., Uppala, S. M., Simmons, A. J., et al. (2011). The ERA-Interim reanalysis: Configuration

and performance. *Quarterly Journal of the Royal Meteorological Society, 137*(656), 553–597.

[8]. De Soto, W., Klein, S. A., & Beckman, W. A. (2006). Improvement and validation of a model for photovoltaic array performance. *Solar Energy, 80*, 78–88.

[9]. Dobos, A., Gilman, P., & Kasberg, M. (2014). P50/P90 analysis for solar energy systems using the System Advisor Model. *IEEE Photovoltaic Specialist Conference*, 668–672.

[10]. Duffie, J. A., & Beckman, W. A. (2013). *Solar engineering of thermal processes* (4th ed.). Wiley.

[11]. Eglen, S. J., Marwick, B., Halchenko, Y. O., et al. (2017). Toward standard practices for sharing reproducible versions of computational research. *eLife, 6*, e31658.

[12]. Espinar, B., Ramirez, L., Drews, A., et al. (2009). Analysis of different comparison parameters applied to solar radiation data. *Solar Energy, 83*(7), 1194–1203.

[13]. European Commission Joint Research Centre. (2024). *PVGIS 5.3: Release features, datasets and temporal coverage*. Photovoltaic Geographical Information System documentation.

[14]. European Commission Joint Research Centre. (2026). *Photovoltaic Geographical Information System (PVGIS): Solar-radiation and photovoltaic-performance services*.

[15]. Farahmand, M. Z., & Yaghoubi, M. (2020). Evaluation of satellite-based solar-radiation data for Iran: A review. *Renewable and Sustainable Energy Reviews, 126*, 109887.

[16]. Gueymard, C. A. (2012). Clear-sky irradiance predictions for solar resource assessment. *Solar Energy, 86*(10), 2746–2761.

[17]. Holmgren, W. F., Hansen, C. W., & Mikofski, M. A. (2018). pvlib python: A Python package for modelling solar-energy systems. *Journal of Open Source Software, 3*, 884.

[18]. Hollmann, R., Merchant, C. J., Saunders, R., et al. (2013). The ESA climate change initiative: Satellite data records for essential climate variables. *Bulletin of the American Meteorological Society, 94*(10), 1541–1552.

[19]. Huld, T., Müller, R., & Gambardella, A. (2012). A new solar-radiation database for estimating PV performance in Europe and Africa. *Solar Energy, 86*, 1803–1815.

[20]. Ineichen, P. (2016). Validation of models that estimate solar irradiance. *Solar Energy, 132*, 469–476.

[21]. Iqbal, M. (1983). *An introduction to solar radiation*. Academic Press.

[22]. International Energy Agency. (2024). *Renewables 2024: Analysis and forecasts to 2030*. Paris: IEA.

[23]. International Renewable Energy Agency. (2023). *World Energy Transitions Outlook 2023: 1.5°C pathway*. Abu Dhabi: IRENA.

[24]. Journée, M., & Bertrand, C. (2011). Quality control of solar-radiation data within the RMIB solar-measurement network. *Solar Energy, 85*, 72–86.

[25]. Kalnay, E., Kanamitsu, M., Kistler, R., et al. (1996). The NCEP/NCAR 40-year reanalysis project. *Bulletin of the American Meteorological Society, 77*(3), 437–471.

[26]. Kaufman, Y. J., Tanré, D., & Boucher, O. (2002). A satellite view of aerosols in the climate system. *Nature, 419*, 215–223.

[27]. Kottek, M., Grieser, J., Beck, C., Rudolf, B., & Rubel, F. (2006). World map of the Köppen-Geiger climate classification updated. *Meteorologische Zeitschrift, 15*(3), 259–263.

[28]. Maghami, M. R., Hizam, H., Gomes, C., Radzi, M. A., Rezadad, M. I., & Hajighorbani, S. (2016). Power loss due to soiling on solar panels: A review. *Renewable and Sustainable Energy Reviews, 59*, 1307–1316.

[29]. Müller, R., Pfeifroth, U., Träger-Chatterjee, C., Cremer, R., Trentmann, J., & Hollmann, R. (2015). Surface solar radiation data set – Heliosat (SARAH), Edition 1. CM SAF.

[30]. Muneer, T., Younes, S., & Kubie, J. (2004). *Quality control of solar radiation data*. Energy Conversion and Management.

[31]. NASA POWER. (2026). *POWER data methodology, data sources and validation documentation*. NASA Langley Research Center.

[32]. Omar, A. H., Winker, D. M., Kittaka, C., et al. (2009). The CALIPSO automated aerosol classification and lidar ratio selection algorithm. *Journal of Atmospheric and Oceanic Technology, 26*(10), 1994–2014.

[33]. Peng, R. D. (2011). Reproducible research in computational science. *Science, 334*(6060), 1226–1227.

[34]. Pérez, R., Ineichen, P., Seals, R., Michalsky, J., & Stewart, R. (1990). Modelling daylight availability and irradiance components from direct and global irradiance. *Solar Energy, 44*, 271–289.

[35]. Pérez, R., Ineichen, P., Moore, K., et al. (2002). A new operational model for satellite-derived irradiances. *Solar Energy, 73*(5), 307–317.

[36]. Pinker, R. T., & Laszlo, I. (1992). Modeling surface solar irradiance for satellite applications. *Journal of Applied Meteorology, 31*(2), 194–211.

[37]. Plesser, H. E. (2018). Reproducibility vs. replicability: A brief history of a confused terminology. *Frontiers in Neuroinformatics, 11*, 76.

[38]. Remund, J., Wald, L., Lefèvre, M., et al. (2003). Worldwide solar radiation database for PV applications. *Solar Energy, 76*(4), 577–589.

[39]. Rumbayan, M., Abudureyimu, A., & Nagasaka, K. (2012). Mapping solar-energy potential in Indonesia using artificial neural networks and GIS. *Renewable and Sustainable Energy Reviews, 16*, 1437–1449.

[40]. Sandve, G. K., Nekrutenko, A., Taylor, J., & Hovig, E. (2013). Ten simple rules for reproducible computational research. *PLoS Computational Biology, 9*(10), e1003285.

[41]. Sengupta, M., Gotseff, P., Stoffel, T., et al. (2018). National solar radiation database. *NREL Technical Report*.

[42]. Stackhouse, P. W., Chandler, W. S., Zhang, T., et al. (2018). NASA surface meteorology and solar energy dataset. *NASA Technical Report*.
[43]. Stodden, V., Leisch, F., & Peng, R. D. (2016). *Implementing reproducible research*. CRC Press.
[44]. Toledano, C., Wiegner, M., Groß, S., et al. (2007). Aerosol optical depth over desert regions. *Atmospheric Chemistry and Physics, 7*, 1101–1116.
[45]. Wilcox, S. (2011). National solar radiation database 1991–2010 update. *NREL Technical Report*.
[46]. Wilks, D. S. (2011). *Statistical methods in the atmospheric sciences* (3rd ed.). Academic Press.
[47]. Willmott, C. J. (1981). On the validation of models. *Physical Geography, 2*(2), 184–194.
[48]. World Meteorological Organization. (2018). *Guide to instruments and methods of observation (WMO-No. 8)*. Geneva: WMO.
[49]. Yang, D. (2016). Solar radiation on inclined surfaces: Corrections and benchmarks. *Solar Energy, 136*, 288–302.
[50]. Yang, D., Bright, J. M., & Hollands, K. G. T. (2014). Bias correction methods for solar radiation data. *Renewable Energy, 68,* 563–573.
[51]. Zelenka, A., Perez, R., Seals, R., & Renné, D. (1999). Effective accuracy of satellite-derived irradiance. *Solar Energy*, *63*(3), 199–210.
[52]. Zhang, Y., Rossow, W. B., Stackhouse, P. W., et al. (2013). Comparison of satellite-derived surface radiation products. *Journal of Climate, 26*(24), 9735–9751.